



Published in final edited form as:

J Phys Chem A. 2010 August 26; 114(33): 8658–8664. doi:10.1021/jp1010549.

Are Anion/ π Interactions Actually a Case of Simple Charge–Dipole Interactions?†

Steven E. Wheeler* and K. N. Houk*

Department of Chemistry and Biochemistry, University of California, Los Angeles, California 90095

Abstract

Substituent effects in $\text{Cl}^- \cdots \text{C}_6\text{H}_{6-n}\text{X}_n$ complexes, models for anion/ π interactions, have been examined using density functional theory and robust ab initio methods paired with large basis sets. Predicted interaction energies for 83 model $\text{Cl}^- \cdots \text{C}_6\text{H}_{6-n}\text{X}_n$ complexes span almost 40 kcal mol⁻¹ and show an excellent correlation ($r = 0.99$) with computed electrostatic potentials. In contrast to prevailing models of anion/ π interactions, which rely on substituent-induced changes in the aryl π -system, it is shown that substituent effects in these systems are due mostly to direct interactions between the anion and the substituents. Specifically, interaction energies for $\text{Cl}^- \cdots \text{C}_6\text{H}_{6-n}\text{X}_n$ complexes are recovered using a model system in which the substituents are isolated from the aromatic ring and π -resonance effects are impossible. Additionally, accurate potential energy curves for Cl^- interacting with prototypical anion-binding arenes can be qualitatively reproduced by adding a classical charge–dipole interaction to the $\text{Cl}^- \cdots \text{C}_6\text{H}_6$ interaction potential. In substituted benzenes, binding of anions arises primarily from interactions of the anion with the local dipoles induced by the substituents, not changes in the interaction with the aromatic ring itself. When designing anion-binding motifs, phenyl rings should be viewed as a scaffold upon which appropriate substituents can be placed, because there are no attractive interactions between anions and the aryl π -system of substituted benzenes.

I. Introduction

There has been a surge of interest in anion/ π interactions in the last five years,^{1–4} leading some authors to list these effects among the pantheon of noncovalent interactions with aromatic rings (i.e., π -stacking, X–H/ π , and cation/ π interactions).⁵ These noncovalent interactions play vital roles in disparate areas of modern chemistry ranging from materials science and supramolecular chemistry to molecular biology. Substituent effects are often used to tune these interactions, providing, among other things, a means of controlling the intermolecular interactions that underlie supramolecular self-assembly phenomena.⁵

Attractive interactions between anions and arenes have a rich history spanning the last century.^{2,4,6} The possibility of favorable noncovalent interactions between an anion and the face of an aromatic ring was largely ignored for many years due to the expected electrostatic repulsion between the anion and the arene π -system. However, recent theoretical studies and mounting experimental evidence of attractive anion–arene interactions have spurred

†Part of the “Klaus Ruedenberg Festschrift”.

© 2010 American Chemical Society

*Corresponding authors, houk@chem.ucla.edu and swhee2@chem.ucla.edu.

Supporting Information Available: Absolute energies, Cartesian coordinates, interaction energies for model systems, and a plot of M06-2X versus CCSD(T) interaction energies. This material is available free of charge via the Internet at <http://pubs.acs.org>.

renewed interest in these interactions in general and those in which the anion appears to interact with the face of an electron-deficient arene in particular.^{1–4,7–10} Enthusiasm for these so-called anion/ π interactions erupted with the experimental demonstration of attractive interactions between Cl^- and pyridine by Reedijk and co-workers¹¹ and between chloride ions and triazine by Meyer et al.,¹² both in 2004. This precipitated countless reports of anion/ π interactions in crystal structures (see refs 1–4 for reviews) and the publication of a bevy of theoretical studies of model anion/ π complexes.^{9,10,13–20} The recent report by Reedijk and co-workers³ of anion/ π interactions in biological systems has engendered further enthusiasm for these interactions.

Analyses of anion–arene contacts in the Cambridge Structural Database (CSD) have led to conflicting conclusions regarding the ubiquity of anion/ π interactions in the solid state.^{10,16,21,22} In 2003, Ahuja and Samuelson concluded²¹ that anion/ π complexes involving six-member aryl rings are rare based on an analysis of interactions of NO_3^- , ClO_4^- , BF_4^- , and BF_6^- with aromatic rings in the CSD. Reedijk and co-workers²² reached markedly different conclusions based on their 2008 analysis of the CSD, finding that “anion– π contacts in fact are quite common supramolecular bonding interactions.” Reedijk et al. even reported²² that there were considerably more examples of anion/ π interactions in the CSD than cation/ π interactions! Hay and Custelcean presented²³ an exhaustive statistical analysis of anion–arene contact in the CSD, finding no “convincing crystal structure evidence for anion– π interactions involving charge neutral, six-member rings with Cl^- , Br^- , I^- , NO_3^- , ClO_4^- , BF_4^- , and PF_6^- anions.” The data revealed that in complexes of anions with neutral six-member aromatic rings the anion was much more likely to engage in aryl C–H hydrogen bonding interactions than anion/ π interactions. Complexes in which the anion is located above the centroid of a substituted benzene ring, the hallmark of an anion/ π interaction, were found to be exceptional.²³

Gas-phase spectroscopic studies^{24,25} and some ab initio computations^{2,8,13} support the findings of Hay and co-workers.²³ For example, Weber and co-workers²⁴ studied the competition between aryl C–H $\cdots \text{X}^-$ and anion/ π interactions in complexes of Cl^- , I^- , and SF_6^- with fluorinated benzenes via infrared photodissociation spectroscopy. Only by replacing all six aryl hydrogens with fluorines could anions be cajoled into complexing with the ring face. As long as at least one aryl hydrogen was present, C–H $\cdots \text{X}^-$ complexes were favored over anion/ π complexes. The ab initio studies of Hay, Johnson, and co-workers^{2,13} and Mascial et al.⁸ similarly predict that C–H hydrogen bonding interactions are favored over anion/ π interactions in complexes of Cl^- with 1,3,5-triazine. Chiavarino et al.²⁵ reported spectroscopic evidence of two binding motifs for complexes of trinitrobenzene and simple anions. These corresponded to weak and strong σ -complexes, not anion/ π complexes.

Complexes of halide anions (usually F^- or Cl^-) and substituted benzenes, in which the halide ion lies above the ring centroid (see Figure 1a), are among the model systems most often invoked to study anion/ π interactions computationally. Previously studied substituted benzenes are depicted in Figure 1b.^{9,10,13–19,26} Among these, studies of C_6F_6 predominate,^{9,10,13–17} although nitrile, nitro, ethynyl, and halo substituted benzenes have also been considered.^{18,19,26} Benzene itself has even been reported to bind halide anions.^{15,19,27} To our knowledge, there has been no systematic study of the effects of more diverse substituents on the binding of halide anions by substituted benzenes.

The approach of a negatively charged halide along the C_6 symmetry axis of benzene is expected to be energetically unfavorable due to repulsive electrostatic interactions, although polarization/induction¹⁵ and dispersion effects can partially compensate this repulsion (vide infra). However, upon attaching electron-withdrawing substituents (e.g., CN, NO_2 , etc.), the interaction of an anion above the arene can become attractive. Invariably, the concept of π -

electron deficient aromatic rings is used to explain the resulting attractive anion/ π interaction.^{1,3,4,9,11,24,26} The prevailing view is that attractive interactions between anions and substituted benzenes arise from the polarization of the benzene π -system by the substituents and subsequent attenuation of the electrostatic repulsion between the halide ion and aromatic π -electron cloud. These explanations are purportedly supported by plots of molecular electrostatic potentials (ESPs),²⁸ which tend to exhibit positive values above the aryl ring in the case of anion-binding arenes. This π -polarization-based model is reminiscent of popular models of substituent effects in π -stacking interactions^{5,29} and is based on the widespread (but false!)³⁰ assumption that changes in the ESP above aromatic rings necessarily reflect changes in the π -electron density.

It will be shown below that binding in $\text{Cl}^- \cdots \text{C}_6\text{H}_{6-n}\text{X}_n$ complexes arises mostly from interactions of chloride with the local dipoles induced by the substituents, not through interactions between the halide ion and the phenyl ring itself. Interactions between the anion and the π -cloud of the phenyl ring remain unfavorable, regardless of the substituents.

II. Theoretical Methods

To enable a thorough examination of substituent effects in $\text{Cl}^- \cdots \text{C}_6\text{H}_{6-n}\text{X}_n$ complexes ($n = 0-4, 6$), we consider a set of 24 diverse substituents ranging from strong electron-donating groups (e.g., $\text{X} = \text{NHCH}_3, \text{NH}_2$) to strong electron acceptors (e.g., $\text{X} = \text{CN}, \text{NO}_2$, etc.). For many of the substituents, steric factors limit the number of possible substitutions. Consequently, for the 1,2,4,5-tetrasubstituted and hexasubstituted phenyl rings, only $\text{X} = \text{CCH}, \text{CH}_3, \text{CN}, \text{F}$, and NH_2 were considered. The full set of substituents was utilized in the monosubstituted, 1,4-disubstituted, and 1,3,5-trisubstituted systems. Due to steric interactions in the tetra- and hexasubstituted systems, the relative orientation of the substituents is not always the same as in the less-substituted species. This leads to nonsystematic behavior in predicted interaction energies for some substituents (e.g., $\text{X} = \text{NH}_2$). In all cases, the lowest-energy conformation was utilized and the anion located above the face of the aryl ring that yields the lowest energy. In total, 83 $\text{Cl}^- \cdots \text{C}_6\text{H}_{6-n}\text{X}_n$ complexes were considered.

Binding energies (Table 1) were computed at the M06-2X/6-31+G(d) level of theory by scanning the distance between Cl^- and the ring centroid (defined here as the center of mass of the benzene carbons) at 0.05 Å increments with the geometry of the substituted benzene frozen at the M05-2X/6-31+G(d) optimized geometry. These M05-2X optimized arene geometries are very similar to M06-2X optimized structures, and their use will have no impact on the predicted interaction energies. The reported interaction energy is the minimum energy obtained along these rigid-monomer scans. Surprisingly, all of the computed interaction potentials exhibited an energy minimum along these scans, although for some substituents this minimum is energetically unstable with respect to the dissociation limit. These complexes are employed as model systems to understand the role of substituent effects; few of the computed structures are energy minima on the unconstrained potential energy surface (PES). To determine which of these complexes are minima on the frozen-monomer PES, single point M06-2X energies were computed with Cl^- displaced from the equilibrium position by ± 0.1 Å along the x and y axes.

To assess the accuracy of the M06-2X interaction energies, estimated CCSD(T)/AVTZ energies were computed at the optimized M06-2X geometries for the monosubstituted complexes, where in general AVXZ denotes the aug-cc-pVXZ basis set.³¹ CCSD(T)/AVTZ energies were estimated by appending a basis set correction at the MP2 level to the

CCSD(T)/AVDZ energy, $E_{\text{AVTZ}}^{\text{CCSD(T)}} \approx E_{\text{AVDZ}}^{\text{CCSD(T)}} + E_{\text{AVTZ}}^{\text{MP2}} - E_{\text{AVDZ}}^{\text{MP2}}$. For selected systems, full CCSD(T)/AVTZ or estimated CCSD(T)/AVTZ one-dimensional potential energy scans

were executed, with the geometry of the substituted benzene fixed at the MP2/AVTZ optimized structure. All ab initio energies employed the frozen-core approximation and were partially corrected for basis-set superposition error (BSSE) via the counterpoise correction.³² The M06-2X energies were not BSSE-corrected.

Nonresonance substituent effects (i.e., inductive/field effects) were evaluated using a simple additive model, depicted in Figure 1c. Similar models have been employed to study substituent effects in the benzene dimer^{33,34} and model cation/ π interactions.³⁵ In this case, the model was constructed by taking the optimized $\text{Cl}^- \cdots \text{C}_6\text{H}_5\text{X}$ complex and replacing the aryl ring with a hydrogen atom. The H atom was placed along the C–X bond and the H–X distance optimized while holding the remaining atoms fixed in space. The resulting $\text{Cl}^- \cdots \text{H-X}$ interaction energy was added to the $\text{Cl}^- \cdots \text{C}_6\text{H}_6$ interaction energy evaluated at the corresponding Cl \cdots centroid distance. The effect of the “extra” two hydrogen atoms was approximately accounted for by subtracting the interaction energy of Cl^- with H_2 at the appropriate distance. In the case of the polysubstituted benzenes, this procedure was carried out for each of the substituents independently, i.e.

$$E_{\text{int}}^{\text{additive}}(\text{Cl}^- \cdots \text{C}_6\text{H}_{6-n}\text{X}_n) = E_{\text{int}}(\text{Cl}^- \cdots \text{C}_6\text{H}_6) + nE_{\text{int}}(\text{Cl}^- \cdots \text{HX}) - nE_{\text{int}}(\text{Cl}^- \cdots \text{HH}) \quad (1)$$

The resulting additive interaction energy should provide an estimate of the inductive/field effects of the substituent on the Cl^- binding energy. Most importantly, in this model the substituent can have no effect on the aryl π -system, because the substituent is separated from the aryl ring.

All M06-2X computations and MP2 optimizations were carried out using NWChem,³⁶ while the MP2 and CCSD(T) energies were evaluated with Molpro 2006.³⁷ A fine DFT quadrature grid, with 70 radial and 590 angular points, was used for the M06-2X computations, because this functional has been shown to be sensitive to integration grid density.³⁸

III. Results and Discussion

A. $\text{F}^- \cdots \text{C}_6\text{H}_6$ and $\text{Cl}^- \cdots \text{C}_6\text{H}_6$ Complexes

In 2006, Clements and Lewis published the provocative prediction²⁷ that benzene can bind halide anions along the C_6 symmetry axis, despite the expected electrostatic repulsion between the anion and the benzene quadrupole moment. Although energetically unstable with respect to separated F^- and C_6H_6 , at the BSSE-corrected MP2/6-311++G** level of theory there is a bound minimum with F^- located 3.2 Å above the ring centroid. Once thermal effects were included, Clements and Lewis predicted a 298 K binding enthalpy of $-0.2 \text{ kcal mol}^{-1}$. Deyà and co-workers¹⁵ more recently presented RI-MP2/6-311++G** computations indicating the presence of minimum energy complexes of benzene with F^- , Cl^- , and Br^- lying 2.8, 2.4, and 1.9 kcal mol^{-1} above the dissociation limit, respectively. More recent BSSE-corrected SCS-RI-MP2/AVTZ' computations from that research group¹⁹ predict binding energies of 1.5 and 1.1 kcal mol^{-1} for F^- and Cl^- with benzene, respectively.

Counterpoise-corrected CCSD(T)/AVTZ potential energy curves for $\text{F}^- \cdots \text{C}_6\text{H}_6$ and $\text{Cl}^- \cdots \text{C}_6\text{H}_6$ complexes with the halide ion lying on the C_6 symmetry axis are shown in Figure 2. Estimated CCSD(T)/AVTZ potential energy curves are also included (dashed curves), demonstrating the accuracy of the MP2 basis set correction across the potential energy surface. There are local minima on these PES curves, corresponding to separations of 3.2 and 3.9 Å for F^- and Cl^- , respectively. These minima are 1.0 and 0.9 kcal mol^{-1} above the dissociation limit and are separated from the dissociated limit by barriers of 0.6 and 0.3 kcal

mol⁻¹, respectively. However, at the CCSD(T)/AVTZ level of theory these configurations are energy *maxima* with respect to displacement of the halide ion away from the C₆ symmetry axis. The minima in Figure 2 are second-order saddle points on the full PESs and are not predicted to be stable in the gas phase.

Beyond 6 Å, the two computed interaction potentials decay in concert, indicating that charge–quadrupole interactions, which will be the same for F⁻ and Cl⁻, dominate at long range, as expected.^{1,10,15–17,26,27} However, the presence of minima on these potential energy curves underscores the fact that anion–arene interactions cannot be even qualitatively described by charge–quadrupole interactions alone. Deyà and co-workers^{15,19} attributed these energy minima to anion-induced polarization effects overwhelming the repulsive electrostatic interactions. Hartree–Fock potential energy curves are displayed in Figure 2 (dashed/dotted lines). For both F⁻ and Cl⁻ above the face of benzene, HF predicts purely repulsive potentials that lie well above the corresponding CCSD(T) potential energy curves, despite the fact that HF will recover the effects of anion-induced polarization.³⁹ Instead, the minima on these potential energy curves must arise from dispersion interactions, which can only be described at correlated levels of theory.

B. Substituent Effects in Cl⁻ ••• C₆H_{6-n}X_n Complexes

M06-2X/6–31+G(d) interaction energies have been evaluated for 83 Cl⁻ ••• C₆H_{6-n}X_n complexes with the Cl⁻ directly above the ring centroid. Interaction energies and the corresponding equilibrium separations (*R_e*) are listed in Table 1. The first observation is that M06-2X/6–31+G(d) predicts that all of the substituted benzenes yield a bound potential for Cl⁻ approaching along the C₆ symmetry axis, with *R_e* values ranging from 2.95 to 3.95 Å. As in the Cl⁻ ••• C₆H₆ complex, some of these minima arise from stabilizing dispersion interactions that overcome repulsive electrostatic effects. Many of these minima lie above the dissociation limit, and only 17 are predicted to be energy minima on the full PESs. Very few substituted benzenes are predicted to bind Cl⁻ above the ring centroid in the gas phase.

Estimated CCSD(T)/AVTZ interaction energies for Cl⁻ above benzene and the monosubstituted benzenes are also included in Table 1. Overall, M06-2X provides an excellent description of these interactions compared to CCSD(T). There is an excellent correlation between the M06-2X/6–31+G(d) and CCSD(T)/AVTZ results (correlation coefficient *r* = 0.998, see Figure S1 in Supporting Information), and M06-2X provides a very reliable but computationally inexpensive means of predicting interaction energies of Cl⁻ with the face of substituted benzenes.

M06-2X predicted interaction energies for the full set of Cl⁻ ••• C₆H_{6-n}X_n complexes span almost 40 kcal mol⁻¹ and are plotted in Figure 3 versus the electrostatic potential (ESP) evaluated at a distance *R_e* above the ring centroid. Estimated CCSD(T)/AVTZ energies are also included and exhibit the same overall trend. As in cation/π interactions,^{35,40} there is a very strong correlation (*r* = 0.99) between the ESP above the ring and computed interaction energies. From the best-fit line, which has a slope very close to unity, a relatively constant stabilizing contribution of -7.1 kcal mol⁻¹ can be attributed to nonelectrostatic effects (i.e., dispersion and polarization/induction). In other words, substituted benzenes are expected to exhibit energetically favorable Cl⁻ binding above the ring centroid as long as the electrostatic potential at that point is below 7.1 kcal mol⁻¹. There are deviations from the best fit line for some of these systems. However, overall, substituent effects in Cl⁻ ••• C₆H_{6-n}X_n complexes arise from electrostatic interactions, and computed ESPs should provide a faithful predictor of anion binding energies across a broad range of substituted arenes.

Deyà and co-workers showed²⁶ a correlation between computed interaction energies of Cl^- with several arenes and the Q_{zz} component of the arene quadrupole moment, which are central to many discussions of anion/ π interactions in the literature.^{1,10,15-17,27} M06-2X and estimated CCSD(T)/AVTZ interaction energies are plotted against M06-2X predicted Q_{zz} values in Figure 3b.⁴¹ There is a correlation ($r = 0.90$), but there is also significantly more scatter in the data than in the plot of E_{int} versus ESP values. Deviations from the linear fit are particularly pronounced for the ethynylbenzenes. For example, the Q_{zz} values for triethynylbenzene, tetraethynylbenzene, and hexaethynylbenzene are -17.0 , -21.4 , and -30.6 B, while the interaction energies with Cl^- change only slightly across this series (-3.0 , -3.4 , -4.3 kcal mol⁻¹, respectively). The computed ESPs above these ethynylbenzenes (-5.6 , -5.8 , -6.3 kcal mol⁻¹, respectively) are much more consistent with the predicted interaction energies.

The relatively poor correlation between Q_{zz} and E_{int} arises in part because the expansion of intermolecular electrostatic interactions in terms of electric multipoles is only valid for well-separated, nonoverlapping charge distributions.⁴² The equilibrium halide–arene distances in $\text{Cl}^- \cdots \text{C}_6\text{H}_{6-n}\text{X}_n$ complexes (2.95–3.95 Å) are too small for multipole expansions to be valid or highly accurate, particularly if only the leading contribution (i.e., charge–quadrupole interaction) is considered. ESP values computed at a point above the ring centroid provide a much more accurate and theoretically sound descriptor of the electrostatic component of anion/ π interactions.

C. Origin of Substituent Effects in $\text{Cl}^- \cdots \text{C}_6\text{H}_{6-n}\text{X}_n$ Complexes

The prevailing view of substituent effects in $\text{Cl}^- \cdots \text{C}_6\text{H}_{6-n}\text{X}_n$ complexes assumes that the interaction is modulated through the polarization of the benzene π -system by the substituents.^{1,3,4,9,11,24,26} To test this, model systems are considered through which the nonresonance component (i.e., field/inductive effects) can be quantified. M06-2X and CCSD(T) interaction energies for the $\text{Cl}^- \cdots \text{C}_6\text{H}_{6-n}\text{X}_n$ complexes are plotted against interaction energies from a simple additive model (eq 1) in Figure 4. There is a good correlation ($r = 0.92$) between the interaction energies in the intact $\text{Cl}^- \cdots \text{C}_6\text{H}_{6-n}\text{X}_n$ complexes and this additive model, despite the fact that no polarization of the aryl π -system is possible in this model. On average, this simple additive model overestimates the interaction energies of $\text{Cl}^- \cdots \text{C}_6\text{H}_{6-n}\text{X}_n$ complexes but captures the overall trend. Substituent effects in $\text{Cl}^- \cdots \text{C}_6\text{H}_{6-n}\text{X}_n$ complexes are not due to π -polarization effects but are instead most readily explained by direct interactions between the substituents and the halide anions. This is in accord with recent models of substituent effects in the sandwich^{33,43} and edge-to-face³⁴ configurations of the benzene dimer, as well as cation/ π interactions.³⁵

To gauge the applicability of this simple model at configurations removed from the equilibrium geometry, potential energy curves for Cl^- interacting with prototypical anion binding arenes are examined using robust ab initio methods. A simpler model, in which the effect of substituents is described by a classical charge–dipole interaction, is also considered, to provide additional physical insight into the origin of these substituent effects. Estimated CCSD(T)/AVTZ potential energy curves for Cl^- above 1,2,4,5-tetracyanobenzene, 1,3,5-trinitrobenzene, and hexafluorobenzene are plotted in Figure 5 versus the distance between Cl^- and the ring centroid (black curves). Also included in each plot is the interaction of Cl^- with $n(\text{HX})$ ($X = \text{CN}$, NO_2 , or F , respectively), $n(\text{HH})$, and C_6H_6 , as well as the curve resulting from combining these three curves as done above (i.e., $\text{Cl}^- \cdots \text{C}_6\text{H}_6 + n(\text{Cl}^- \cdots \text{HX}) - n(\text{Cl}^- \cdots \text{HH})$, red dashed curves). For tetracyanobenzene and trinitrobenzene, these additive potential energy curves slightly overestimate the explicitly computed $\text{Cl}^- \cdots \text{C}_6\text{H}_{6-n}\text{X}_n$ interaction energies. For C_6F_6 the overbinding is more severe. This is because in C_6F_6 the fluorines donate π -electron density to the aryl ring,

partially compensating the effects of σ -electron withdrawal. This is consistent with the traditional characterization of fluorine as a strong σ -electron acceptor but π -electron donor (e.g., the field and resonance parameters for F are 0.45 and -0.39 , respectively).⁴⁴ In the $\text{Cl}^- \cdots \text{C}_6\text{F}_6$ complex, the σ -withdrawing effect of the fluorines increase the binding energy significantly, but this effect is tempered by the π -donation of the fluorines. This π -donation effect is not possible in the additive model. The π -accepting effects of CN and NO_2 will also be neglected in the additive model, yet the additive interaction curves for $\text{C}_6\text{H}_2(\text{CN})_4$ and $\text{C}_6\text{H}_3(\text{NO}_2)_3$ are in qualitative agreement with the explicitly computed potentials, demonstrating that in these cases π -accepting effects are not the root of the substituent effects on anion binding.

The solid blue curves in Figure 5 depict the interaction of a point charge (at a distance R above the ring centroid) with idealized point dipoles located at the centers of mass of the substituents. The sizes of these dipoles are equal to the MP2/AVTZ predicted dipole moments of the corresponding H-X species (HCN, 3.02 D; HF, 1.81 D; HNO_2 , 2.56 D). These charge-dipole interactions were added to the $\text{Cl}^- \cdots \text{C}_6\text{H}_6$ potential curve to yield the blue dashed curves. This model captures the substituent effect on Cl^- binding due solely to the interaction of the anion with the local dipole induced by the substituent. In each case, the blue dashed curve lies above the curve from the additive model (red dashed curve), because in the additive model there will be polarization/induction and dispersion interactions between the anion and substituents, in addition to charge-dipole interactions. For tetracyanobenzene and trinitrobenzene, the charge-dipole model slightly underestimates the explicitly computed interaction potential due to this lack of dispersion and polarization/induction effects. For C_6F_6 , this charge-dipole model predicts a more deeply bound potential energy curve than that computed for the intact system, again due to the π -donation effects of fluorine in the intact system. In these systems, the dominant factor leading to Cl^- binding is the interaction of the anion with the local dipoles created by the substituents. In each case, the interaction of Cl^- with the aryl ring itself remains unfavorable, regardless of the nature of the substituents.

IV. Summary and Conclusions

The effect of substituents on the ability of benzene to bind Cl^- above the ring centroid has been examined. Surprisingly, all $\text{Cl}^- \cdots \text{C}_6\text{H}_{6-n}\text{X}_n$ complexes are predicted to yield bound potentials for the anion above the ring centroid. However, some of these stationary points lie above the dissociation limit and only 17 of 83 complexes studied are predicted to be stable minima on the frozen monomer M06-2X/6-31+G(d) PES. In all of these systems, substituent effects are primarily electrostatic, and predicted interaction energies correlate very well with computed ESPs above the ring centroid.

Conventional explanations^{1,3,4,9,11,24,26} of the attractive interactions between anions and substituted benzenes, which hinge on the substituent-induced polarization of the aryl π system, are flawed. Instead, it was shown that anion binding arises primarily from the direct interaction of the anion with the local dipoles induced by the substituents, as depicted in Figure 6. The interaction of the anion with the aromatic ring itself remains energetically unfavorable, despite the substituents. Specifically, interaction energies for a set of 83 $\text{Cl}^- \cdots \text{C}_6\text{H}_{6-n}\text{X}_n$ complexes ($n = 0-4, 6$) can be qualitatively reproduced using a simple additive model in which the substituents are not connected to the aromatic ring and π -polarization effects are impossible. Additionally, for tetracyanobenzene and trinitrobenzene, CCSD(T) potential energy curves are well described by adding a classical charge-dipole interaction to the $\text{Cl}^- \cdots \text{C}_6\text{H}_6$ potential curve. In all of these systems, the binding arises because the repulsive interaction between the anion and the arene is overcome by favorable charge-dipole and other direct interactions between the anion and the substituents. Substituted

benzenes do not bind anions because of favorable interactions with the aryl π -systems, but despite the π -systems. These results offer an explanation of the finding of Hay and Custelcean²³ that anions are unlikely to bind above the center of substituted aryl rings. It should be noted, however, that the present results apply only to substituted benzenes, and the origin of anion binding by heterocyclic aromatics remains an open question.

Regarding the rational design of anion receptors, the present results indicate that phenyl rings should be viewed simply as scaffolds upon which appropriate substituents can be positioned to yield favorable charge–dipole interactions. This can be demonstrated by comparing the interaction of Cl^- with benzene, cyclohexane, and their nitrile-substituted analogues (see Figure 7). M06-2X/6–31+G(d) predicted interaction energies are plotted in Figure 7 as a function of the distance of the anion above the ring centroid for these four systems. In both benzene and cyclohexane, the introduction of CN induces a dramatic increase in the interaction energy, despite the lack of a polarizable π system in cyclohexane, because in both systems the increased binding arises from simple charge–dipole interactions.

Supplementary Material

Refer to Web version on PubMed Central for supplementary material.

Acknowledgments

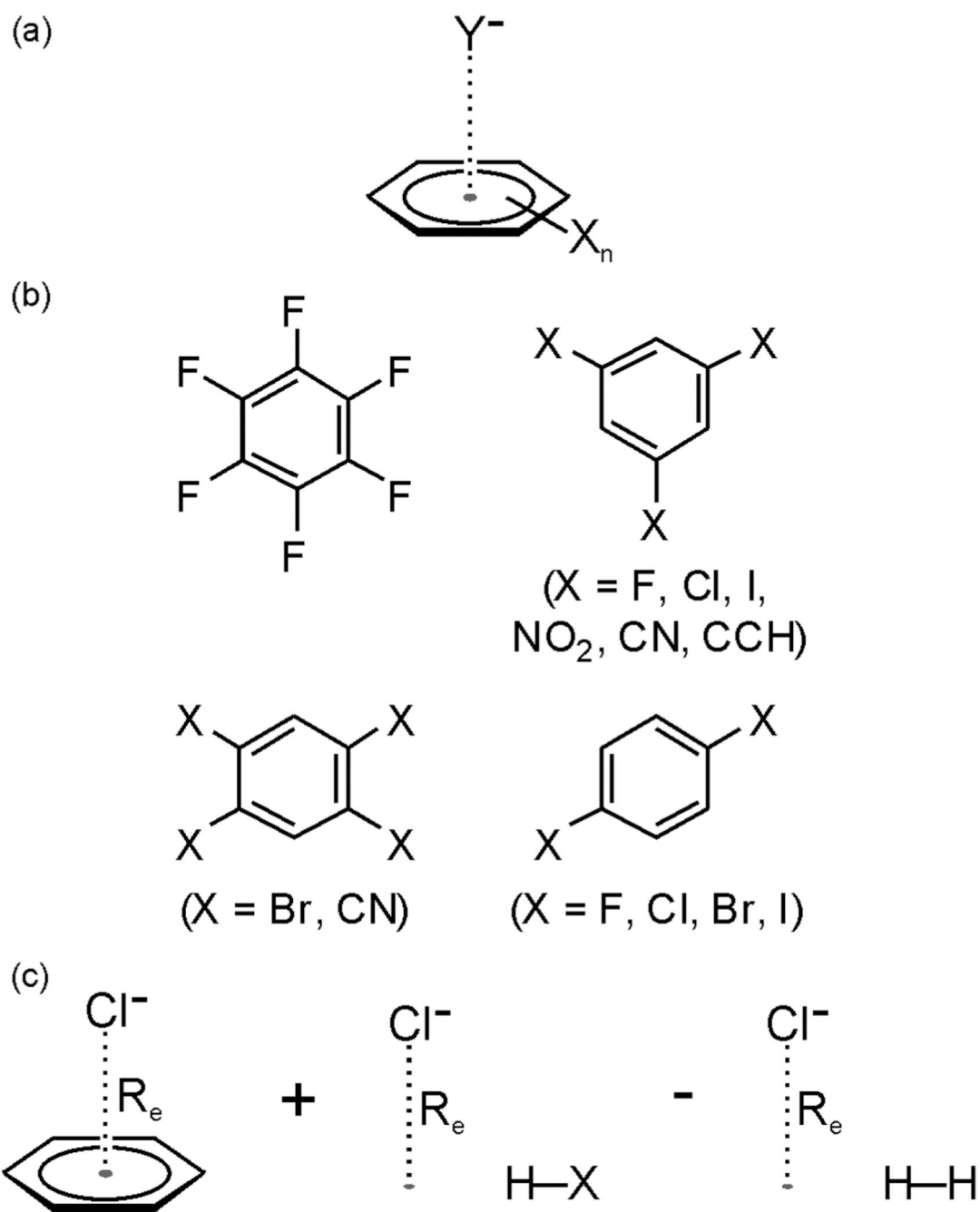
This work was supported by the National Institutes of General Medical Sciences NRSA Postdoctoral Fellowship F32 GM082114 (S.E.W.) and R01 GM036700 (K.N.H.). S.E.W. thanks S. J. Klippenstein for fruitful discussions and K. R. Dunbar and B. P. Hay for helpful comments regarding the manuscript. Computer time was provided by the UCLA Institute for Digital Research and Education (IDRE).

References and Notes

1. Ballester P. *Struct. Bonding* (Berlin) 2008;129:127. Schottel BL, Chifotides HT, Dunbar KR. *Chem. Soc. Rev* 2008;37:68. [PubMed: 18197334]
2. Hay BP, Bryantsev VS. *Chem. Commun* 2008:2417.
3. Gamez P, Mooibroek TJ, Teat SJ, Reedijk J. *Acc. Chem. Res* 2007;40:435. [PubMed: 17439191]
4. Berryman OB, Johnson DW. *Chem. Commun* 2009:3143.
5. Meyer EA, Castellano RK, Diederich F. *Angew. Chem. Int. Ed* 2003;42:1210.
6. Jackson CL, Boos WF. *Am. Chem. J* 1898;20:444. Jackson CL, Gazzolo FH. *Am. Chem. J* 1900;23:376. Meisenheimer J. *Liebigs Ann. Chem* 1902;323:205. Kebarle P, Chowdhury S. *Chem. Rev* 1987;87:513. Paul GJC, Kebarle P. *J. Am. Chem. Soc* 1991;113:1148.
7. Chowdhury S, Kebarle P. *J. Chem. Phys* 1986;85:4989. Hiraoka K, Mizuse S, Yamabe S. *J. Phys. Chem* 1987;91:5294. Schneider H-J, Werner F, Blatter T. *J. Phys. Org. Chem* 1993;6:590.
8. Mascall M, Armstrong A, Bartberger MD. *J. Am. Chem. Soc* 2002;124:6274. [PubMed: 12033854]
9. Alkorta I, Rozas I, Elguero J. *J. Am. Chem. Soc* 2002;124:8593. [PubMed: 12121100]
10. Quiñonero D, Garau C, Rotger C, Frontera A, Ballester P, Costa A, Deyà PM. *Angew. Chem. Int. Ed* 2002;41:3389.
11. de Hoog P, Gamez P, Mutikainen H, Turpeinen U, Reedijk J. *Angew. Chem. Int. Ed* 2004;43:5815.
12. Demeshko S, Dechert S, Meyer F. *J. Am. Chem. Soc* 2004;126:4508. [PubMed: 15070355]
13. Berryman OB, Bryantsev VS, Stay DP, Johnson DW, Hay BP. *J. Am. Chem. Soc* 2007;129:48. [PubMed: 17199282]
14. Kim D, Tarakeshwar P, Kim KS. *J. Phys. Chem. A* 2005;108:1250. Garau C, Frontera A, Ballester P, Quiñonero D, Costa A, Deyà PM. *Eur. J. Org. Chem* 2005:179. Quiñonero D, Garau C, Frontera A, Ballester P, Costa A, Deyà PM. *J. Phys. Chem. A* 2005;109:4632. [PubMed: 16833802]
15. Frontera A, Quiñonero D, Costa A, Ballester P, Deyà PM. *New J. Chem* 2007;31:556.

16. Quiñonero D, Garau C, Frontera A, Ballester P, Costa A, Deyà PM. *Chem. Phys. Lett* 2002;359:486.
17. Garau C, Frontera A, Quiñonero D, Ballester P, Costa A, Deyà PM. *Chem. Phys. Lett* 2004;392:85.
18. Garau C, Frontera A, Quiñonero D, Ballester P, Costa A, Deyà PM. *J. Phys. Chem. A* 2004;108:9423. Quiñonero D, Frontera A, Garau C, Ballester P, Costa A, Deyà PM. *ChemPhysChem* 2006;7:2487. [PubMed: 17072938]
19. Lucas X, Quiñonero D, Frontera A, Deyà PM. *J. Phys. Chem. A* 2009;113:10367. [PubMed: 19757849]
20. Garau C, Quiñonero D, Frontera A, Ballester P, Costa A, Deyà PM. *J. Phys. Chem. A* 2005;109:9341. [PubMed: 16833275] Frontera A, Saczewski F, Gdaniec M, Dziemidowicz-Borys E, Kurland A, Deyà PM, Quiñonero D, Garau C. *Chem.-Eur. J* 2005;11:6560. Garau C, Quiñonero D, Frontera A, Escudero D, Ballester P, Costa A, Deyà PM. *Chem. Phys. Lett* 2007;438:104.
21. Ahuja R, Samuelson AG. *CrystEngComm* 2003;5:395.
22. Mooibroek TJ, Black CA, Gamez P, Reedijk J. *Cryst. Growth Des* 2008;8:1082.
23. Hay BP, Custelcean R. *Cryst. Growth Des* 2009;9:2539.
24. Schneider H, Vogelhuber KM, Schinle F, Weber JM. *J. Am. Chem. Soc* 2007;129:13022. [PubMed: 17918835]
25. Chiavarino B, Crestoni ME, Fornarini S, Lanucara F, Lemaire J, Maître P, Scuderi D. *Chem.—Eur. J* 2009;15:8185.
26. Garau C, Frontera A, Quiñonero D, Ballester P, Costa A, Deyà PM. *ChemPhysChem* 2003;4:1344. [PubMed: 14714384]
27. Clements A, Lewis M. *J. Phys. Chem. A* 2006;110:12705. [PubMed: 17107123]
28. Politzer, P.; Truhlar, DG. *Chemical Applications of Atomic and Molecular Electrostatic Potentials*. New York: Plenum; 1981. Murray, JS.; Sen, K. *Molecular Electrostatic Potentials: Concepts and Applications*. Amsterdam and New York: Elsevier Science; 1996. Naráy-Szabó G, Ferenczy GG. *Chem. Rev* 1995;95:829. Politzer, P.; Murray, JS. *Computational Medical Chemistry for Drug Discovery*. Bultinck, P.; De Winter, H.; Langenaeker, W.; Tollenaere, JP., editors. New York: Marcel Dekker, Inc; 2004. p. 213. Politzer, P.; Murray, JS. *The Electrostatic Potential as a Guide to Molecular Interactive behavior*. In: Chattaraj, PK., editor. *Chemical Reactivity Theory: A Density Functional View*. Boca Raton, FL: CRC Press; 2009.
29. Cozzi F, Cinquini M, Annunziata R, Dwyer T, Siegel JS. *J. Am. Chem. Soc* 1992;114:5729. Cozzi F, Siegel JS. *Pure Appl. Chem* 1995;67:683. Cozzi F, Annunziata R, Benaglia M, Cinquini M, Raimondi L, Baldrige KK, Siegel JS. *Org. Biomol. Chem* 2003;1:157. [PubMed: 12929404] Cozzi F, Annunziata R, Benaglia M, Baldrige KK, Aguirre G, Estrada J, Sritana-Anant Y, Siegel JS. *Phys. Chem. Chem. Phys* 2008;10:2686. [PubMed: 18464983] Hunter CA, Sanders JKM. *J. Am. Chem. Soc* 1990;112:5525. Hunter CA, Lawson KR, Perkins J, Urch CJ. *J. Chem. Soc. Perkin Trans* 2001;2:651.
30. Wheeler SE, Houk KN. *J. Chem. Theory Comput* 2009;5:2301. [PubMed: 20161573]
31. Kendall RA, Dunning TH Jr, Harrison RJ. *J. Chem. Phys* 1992;96:6796.
32. Boys SF, Bernardi F. *Mol. Phys* 1970;19:553.
33. Wheeler SE, Houk KN. *J. Am. Chem. Soc* 2008;130:10854. [PubMed: 18652453]
34. Wheeler SE, Houk KN. *Mol. Phys* 2009;107:749. [PubMed: 20046948]
35. Wheeler SE, Houk KN. *J. Am. Chem. Soc* 2009;131:3126. [PubMed: 19219986]
36. Kendall RA, Apra E, Bernholdt DE, Bylaska EJ, Dupuis M, Fann GI, Harrison RJ, Ju J, Nichols JA, Nieplocha J, Straatsma TP, Windus TL, Wong AT. *Comput. Phys. Commun* 2000;128:260. Bylaska, EJ.; de Jong, WA.; Govind, N.; Kowalski, K.; Straatsma, TP.; Valiev, M.; Wang, D.; Aprà, E.; Windus, TL.; Hammond, J.; Nichols, P.; Hirata, S.; Hackler, MT.; Zhao, Y.; Fan, P-D.; Harrison, RJ.; Dupuis, M.; Smith, DMA.; Nieplocha, J.; Tipparaju, V.; Krishnan, M.; Wu, Q.; Van Voorhis, T.; Auer, AA.; Nooijen, M.; Brown, E.; Cisneros, G.; Fann, GI.; Fruchtl, H.; Garza, J.; Hirao, K.; Kendall, R.; Nichols, JA.; Tsemekhman, K.; Wolinski, K.; Anchell, J.; Bernholdt, D.; Borowski, P.; Clark, T.; Clerc, D.; Dachsel, H.; Deegan, M.; Dyall, K.; Elwood, D.; Glendening, E.; Gutowski, M.; Hess, A.; Jaffe, J.; Johnson, B.; Ju, J.; Kobayashi, R.; Kutteh, R.; Lin, Z.; Littlefield, R.; Long, X.; Meng, B.; Nakajima, T.; Niu, S.; Pollack, L.; Rosing, M.;

- Sandrone, G.; Stave, M.; Taylor, H.; Thomas, H.; van Lenthe, J.; Wong, A.; Zhang, Z. NWChem, A Computational Chemistry Package for Parallel Computers. Richland, WA: Pacific Northwest National Laboratory; 2007. Version 5.1
37. Werner H-J, Knowles PJ, Lindh R, Manby FR, Schu'tz M, Celani P, Korona T, Rauhut G, Amos RD, Bernhardsson A, Berning A, Cooper DL, Deegan MJO, Dobbyn AJ, Eckert F, Hampel C, Hetzer G, Lloyd AW, McNicholas SJ, Meyer W, Mura ME, Nicklaß P, Palmieri R, Pitzer U, Schumann H, Stoll H, Stone AJ, Tarroni R, Thorsteinsson T. MOLPRO. version 2006.1; a package of ab initio programs.
38. Johnson ER, Wolkow RA, DiLabio GA. Chem. Phys. Lett 2004;394:334. Johnson ER, Becke A, Sherrill CD, DiLabio GA. J. Chem. Phys 2009;131:034111. [PubMed: 19624185] Gräfenstein J, Cremer D. J. Chem. Phys 2007;127:164113. [PubMed: 17979325] Gräfenstein J, Izotov D, Cremer D. J. Chem. Phys 2007;127:214103. [PubMed: 18067345] Wheeler SE, Houk KN. J. Chem. Theory Comput 2010;6:395. [PubMed: 20305831]
39. The *zz* component of the polarizability tensor of benzene is predicted to be 44.5 and 45.4 au at the CCSD(T)/AVTZ and HF/AVTZ levels of theory, respectively.
40. Mecozi S, West AP Jr, Dougherty DA. Proc. Natl. Acad. Sci. U.S.A 1996;93:10566. [PubMed: 8855218] Ma JC, Dougherty DA. Chem. Rev 1997;97:1303. [PubMed: 11851453] Dougherty DA. Science 1996;271:163. [PubMed: 8539615] Mecozi S, West AP Jr, Dougherty DA. J. Am. Chem. Soc 1996;118:2307.
41. The quadrupole moment tensor was computed with the origin located at the ring centroid and the arene in the *xy*-plane.
42. Hirschfelder, JO.; Curtiss, CF.; Bird, RB. Molecular Theory of Gases and Liquids. New York: John Wiley & Sons; 1954.
43. Wheeler SE, McNeil AJ, Müller P, Swager TM, Houk KN. J. Am. Chem. Soc 2010;132:3304. [PubMed: 20158182]
44. Charton M. Prog. Phys. Org. Chem 1991;13:120. Hansch C, Leo A, Taft RW. Chem. Rev 1991;91:165.

**Figure 1.**

(a) Prototype anion/ π interaction of an halide anions ($Y = \text{F}, \text{Cl}, \text{Br}, \text{or I}$) with a substituted benzene. (b) Previously studied anion-binding substituted benzenes. (c) Additive model used to gauge through-space substituent effects in $\text{Cl}^- \cdots \text{C}_6\text{H}_{6-n}\text{X}_n$ complexes.

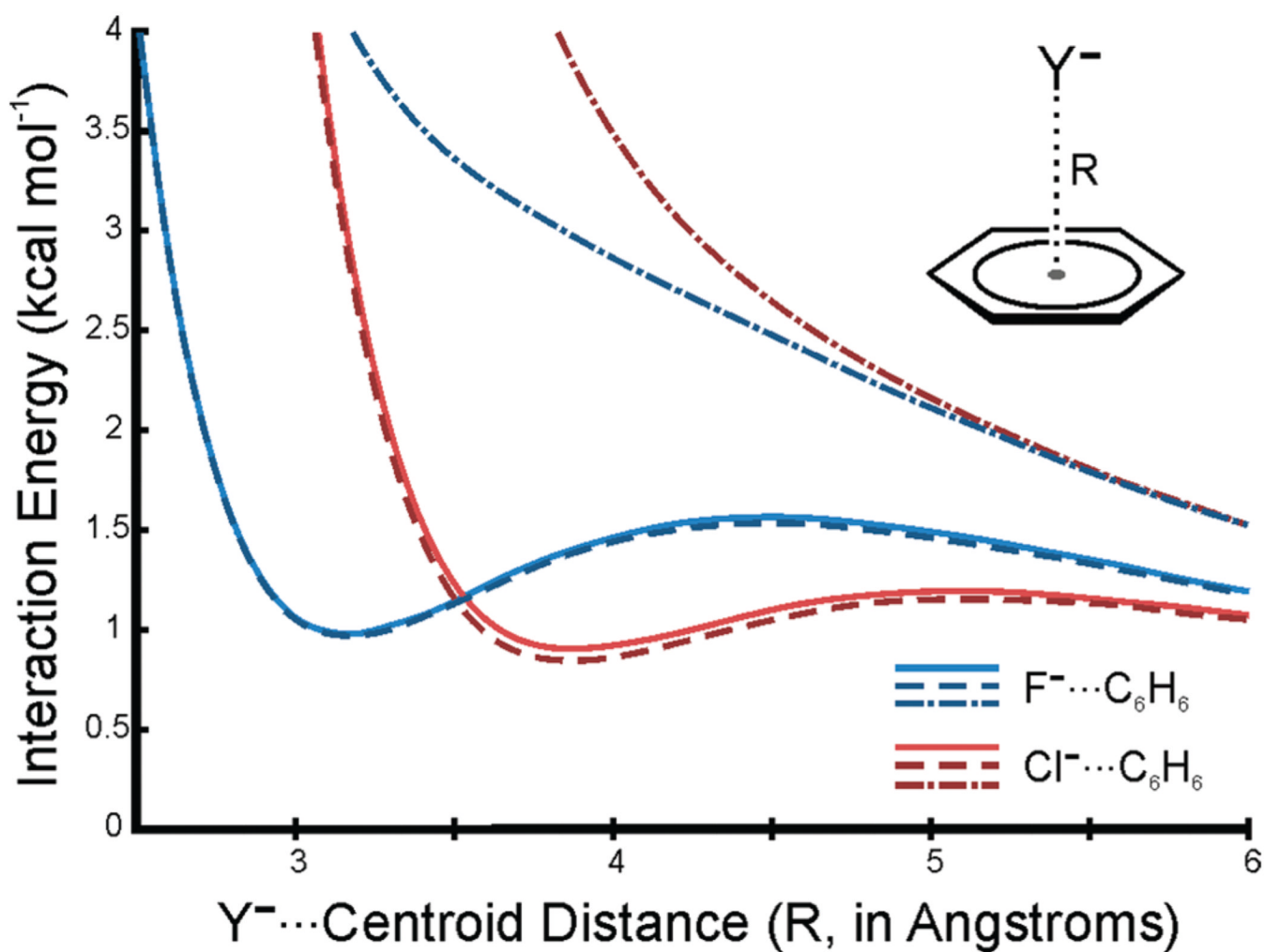


Figure 2. CCSD(T)/AVTZ (solid lines), estimated CCSD(T)/AVTZ (dashed lines), and HF/AVTZ (dashed/dotted lines) potential energy curves (kcal mol⁻¹) for F⁻ ••• C₆H₆ and Cl⁻ ••• C₆H₆ as a function of the anion ••• centroid distance. The minima are second-order saddle points on the full CCSD(T)/AVTZ PES.

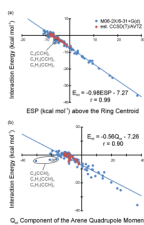


Figure 3. M06-2X/6-31+G(d) and estimated CCSD(T)/AVTZ interaction energies (kcal mol⁻¹) for Cl⁻ ••• C₆H_{6-n}X_n complexes versus (a) the M06-2X electrostatic potential (kcal mol⁻¹) evaluated at the position of Cl⁻ above the ring and (b) the M06-2X predicted Q_{zz} component of the quadrupole moment tensor, in buckinghams. The linear fits are applied to the M06-2X data only.

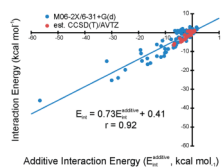


Figure 4. M06-2X/6-31+G(d) and estimated CCSD(T)/AVTZ interaction energies (kcal mol⁻¹) for Cl⁻ ••• C₆H_{6-n}X_n complexes versus the additive interaction energies at the corresponding level of theory (eq 1). The linear fit is applied to the M06-2X data only.

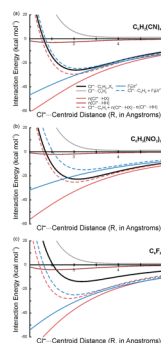


Figure 5. Potential energy scans for Cl^- above the center of (a) tetracyanobenzene, (b) trinitrobenzene, and (c) hexafluorobenzene computed at the estimated CCSD(T)/AVTZ level of theory (black curves) and via two simple additive models (dashed curves). The red dashed curves estimate the substituent effect due to direct interactions of Cl^- with the substituents while in the blue dashed curve the effect of the substituent is captured by a charge-dipole interaction ($\vec{r} \bullet \vec{\mu} / r^3$). In each plot, the estimated CCSD(T)/AVTZ $\text{Cl}^- \cdots \text{C}_6\text{H}_6$ potential energy curve is in gray.

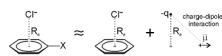


Figure 6. Electrostatic model of substituent effects in $\text{Cl}^- \cdots \text{C}_6\text{H}_{6-n}\text{X}_n$ complexes. Interaction energies of Cl^- with substituted benzenes can be captured by adding an electrostatic charge–dipole interaction to the $\text{Cl}^- \cdots \text{C}_6\text{H}_6$ interaction. The substituents do not effect any significant net change in the interaction of the anion with the aromatic ring itself.

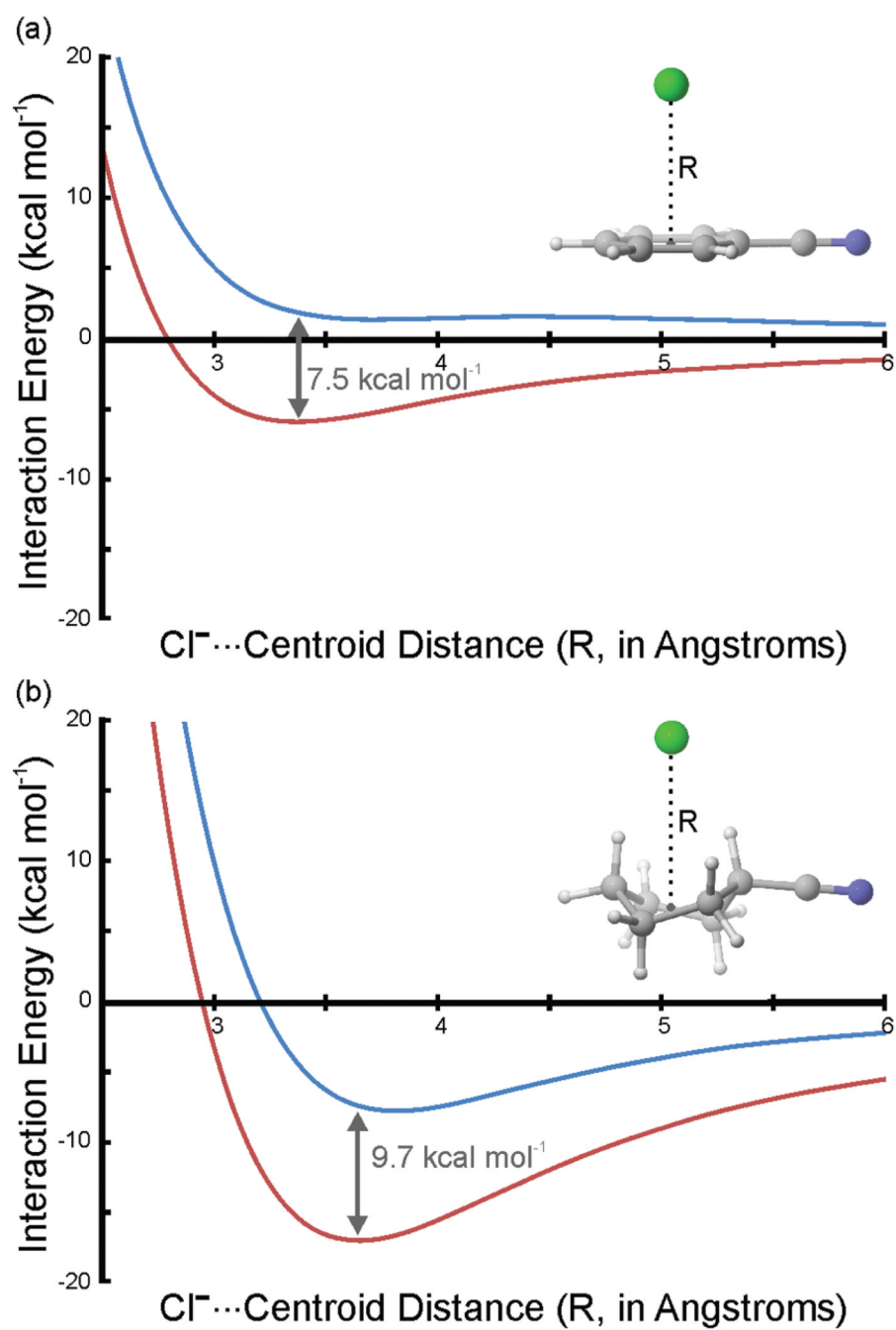


Figure 7. M06-2X/6-31+G(d) interaction energies for Cl⁻ approaching the centroid of (a) benzene (blue curve) and cyanobenzene (red curve) and (b) twist-boat cyclohexane (blue curve) and cyclohexanecarbonitrile (red curve).

TABLE 1
 M06-2X/6-31+G(d) Interaction Energies (kcal mol⁻¹) and Cl ••• Ring Centroid Distances (*R_e*, in Angstroms) for Cl⁻ ••• C₆H_{6-n}X_n Complexes, with the Cl⁻ Constrained to Lie above the Ring Centroid^a

	<i>n</i> = 1		<i>n</i> = 2		<i>n</i> = 3		<i>n</i> = 4		<i>n</i> = 6	
	<i>E</i> _{int}	<i>R_e</i>	<i>E</i> _{int}	<i>R_e</i>	<i>E</i> _{int}	<i>R_e</i>	<i>E</i> _{int}	<i>R_e</i>	<i>E</i> _{int}	<i>R_e</i>
H	1.7 (0.9)	3.75								
CH ₂ OH	2.1 (1.1)	3.70	2.5	3.65	2.8	3.55				
NHOH	1.9 (0.9)	3.70	1.3	3.55	2.0 ^b	3.50				
N(CH ₃) ₂	1.7 (0.7)	3.75	0.3	3.65	1.0	3.70				
NHCH ₃	1.5 (0.6)	3.80	0.1	3.65	1.0	3.75				
OCH ₃	1.4 (0.7)	3.60	0.9	3.60	1.0 ^b	3.50				
OH	1.3(0.6)	3.60	0.6	3.55	0.4 ^b	3.55				
CH ₃	1.1 (0.3)	3.65	0.4	3.60	-0.4 ^b	3.55	-0.1	3.55	-1.0	3.50
NH ₂	1.0 (0.3)	3.75	-0.6	3.70	-0.3	3.75	3.0	3.60	1.5	3.50
SCH ₃	0.8 (-0.1)	3.60	-0.2	3.45	-0.7 ^b	3.40				
SH	0.3(-0.6)	3.55	-1.3	3.45	-2.5 ^b	3.35				
CCH	0.0(-0.7)	3.50	-1.5 ^b	3.40	-3.0 ^b	3.30	-3.4	3.25	-4.3 ^b	3.15
SiH ₃	-0.4 (-1.4)	3.55	-2.4	3.45	-4.5	3.40				
F	-0.8(-1.3)	3.55	-3.6	3.40	-6.3 ^b	3.35	-9.2 ^b	3.25	-15.1 ^b	3.15
COOCH ₃	-1.1 (-1.8)	3.50	-3.6	3.35	-6.2	3.30				
COOH	-1.9 (-2.5)	3.50	-5.2	3.35	-8.7	3.25				
COCH ₃	-2.5(-3.1)	3.45	-6.6	3.35	-10.7	3.25				
OCF ₃	-2.6 (-3.0)	3.45	-7.1	3.30	-11.0 ^b	3.20				
BF ₂	-3.0 (-3.5)	3.50	-7.6	3.35	-12.4 ^b	3.25				
CHO	-3.2 (-3.7)	3.45	-8.0	3.30	-12.9 ^b	3.25				
CF ₃	-3.3 (-3.8)	3.45	-8.5	3.30	-13.7	3.20				
NO	-4.4(-4.6)	3.40	-10.3	3.25	-16.8	3.10				
SiF ₃	-4.5 (-4.9)	3.40	-10.3	3.30	-16.1	3.20				

	$n = 1$		$n = 2$		$n = 3$		$n = 4$		$n = 6$	
	E_{int}	R_e	E_{int}	R_e	E_{int}	R_e	E_{int}	R_e	E_{int}	R_e
CN	-5.3 (-5.8)	3.40	-12.4	3.25	-19.7	3.15	-25.3	3.05	-35.9 ^b	2.95
NO ₂	-6.7 (-6.6)	3.35	-15.2	3.20	-24.0 ^b	3.10				

^a Estimated CCSD(T)/AVTZ//M06-2X/6-31+G(d) interaction energies for the monosubstituted systems are provided in parentheses.

^b Only these systems are predicted to be energy minima on the frozen-monomer M06-2X/6-31+G(d) PES.